# Batch adsorption of methylene blue from aqueous solution by garlic peel, an agricultural waste biomass

B.H. Hameed*, A.A. Ahmad

*School of Chemical Engineering, Engineering Campus, Universiti Sains Malaysia, 14300 Nibong Tebal, Penang, Malaysia*

## ARTICLE INFO

## ABSTRACT

The potential of garlic peel (GP), agricultural waste, to remove methylene blue (MB) from aqueous solution was evaluated in a batch process. Experiments were carried out as function of contact time, initial concentration (25–200 mg/L), pH (4–12) and temperature (303, 313 and 323 K). Adsorption isotherms were modeled with the Langmuir, Freundlich, and Temkin isotherms. The data fitted well with the Freundlich isotherm. The maximum monolayer adsorption capacities were found to be 82.64, 123.45, and 142.86 mg/g at 303, 313, and 323 K, respectively. The kinetic data were analyzed using pseudo-first-order and pseudo-second-order models. The results indicated that the garlic peel could be an alternative for more costly adsorbents used for dye removal.

© 2008 Elsevier B.V. All rights reserved.

## 1. Introduction

Dyes usually have a synthetic origin and complex aromatic molecular structures which make them more stable and more difficult to biodegrade. Today there are more than 10,000 dyes available commercially [1]. Dyes are widely used in textiles, paper, rubber, plastics, leather, cosmetics, pharmaceutical and food industries. The discharge of colored wastewater from these industries into natural streams has caused many significant problems such as increasing the toxicity and chemical oxygen demand (COD) of the effluent, and also reducing light penetration, which has a derogatory effect on photosynthetic phenomena [2]. Methylene blue (MB) has wider applications, which include coloring paper, temporary hair colorant, dyeing cottons, wools, and coating for paper stock. Though methylene blue is not strongly hazardous, it can cause some harmful effects. Acute exposure to methylene blue will cause increased heart rate, vomiting, shock, Heinz body formation, cyanosis, jaundice, quadriplegia, and tissue necrosis in humans [2].

The conventional methods for treating dyes containing wastewaters are coagulation and flocculation [3], oxidation or ozonation [4,5], membrane separation [6] and activated carbon adsorption [7,8]. Currently adsorption on activated carbon is widely used for removal of dyes, but it is still considered expensive adsorbent.

Recently, various low-cost adsorbents derived from agricultural waste or natural materials, have been investigated intensively for dye removal from aqueous solutions. Many researchers have investigated the use of cheap and efficient alternative substitutes to remove dyes from wastewater. Some of these alternative adsorbents are palm ash and chitosan/oil palm ash [9,10], shale oil ash [11], pomelo (*Citrus grandis*) peel [12], de-oiled soya and bottom ash [13], sunflower seed shells and mandarin peelings [14], wheat husk [15,16], guava leaf powder [17] and steel and fertilizer industries wastes [18].

Garlic peel, agricultural and easily available waste, could be an alternative for more costly wastewater treatment processes. Due to the high consumption of garlic, massive amounts of peels are disposed, causing a sever problem in the community. In the interest of the environment, we propose this agricultural waste as a low-cost adsorbent to remove methylene blue from aqueous solution.

The aim of this study was to evaluate the potentiality of garlic peel (GP) for the removal of MB from aqueous solution. The effects of initial dye concentration, contact time, solution pH and temperature on MB adsorption were evaluated.
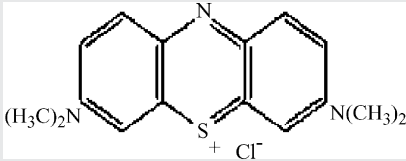
## 2. Materials and methods

### 2.1. Adsorbate

Methylene blue supplied by Sigma–Aldrich (M) Sdn Bhd, Malaysia was used as an adsorbate. The characteristics of the dye

---

* Corresponding author. Fax: +60 4 5941013.
*E-mail address:* chbassim@eng.usm.my (B.H. Hameed).

## Table 1
Properties and characteristics of MB

| | |
|---|---|
| Generic name | Methylene blue |
| Chemical name (IUPAC) | 3,7-bis(Dimethylamino)-phenazathionium chloride tetramethylthionine chloride |
| Chemical formula | $C_{16}H_{18}ClN_3S \cdot 3H_2O$ |
| Molecular weight (g/mol) | 373.90 |
| Molecular volume (cm³/mol) | 241.9 |
| Molecular diameter (nm) | 0.80 |
| $\lambda_{max}$ (nm) | 668 |
| Colour index number | 52,015 |
| Chemical structure | |

are listed in Table 1. Distilled water was used for preparing all solutions.

### 2.2. Preparation and characterization of GP adsorbent

Garlic peels (GP) used in this study was obtained from the vegetable market in Nibong Tebal, Penang, Malaysia. The sample was washed with distilled water, boiled with water for 30 min, filtered out and dried in an oven at 60 °C for 24 h. The dried materials were crushed and sieved to desired mesh size (100–300 μm). The prepared GP sample was stored in an airtight container for further use. No other chemical or physical treatments were used prior to adsorption experiments.

Textural characterization of the GP was carried out by $N_2$ adsorption at 77 K using Autosorb I (Quantachrome Corporation, USA). The surface functional groups of GP were detected by Fourier transform infrared (FTIR) spectroscope FTIR-2000, PerkinElmer. The spectra were recorded from 4000 to 400 cm$^{-1}$. Surface morphology of porosity of the GP were studied using scanning electron microscopy (SEM) analysis.

### 2.3. Batch equilibrium and kinetic studies

Adsorption experiments were carried out by adding a fixed amount of GP (0.30 g) to a series of 250 mL conical flasks filled with 100 mL diluted solutions (25–200 mg/L). The conical flasks were then sealed and placed in a water-bath shaker and shaken at 100 rpm with a required time at 303, 313 and 323 K. The flasks were then removed from the shaker, and the final concentration of dye in the solution was measured at maximum wavelengths of MB (668 nm) using a double beam UV/vis spectrophotometer (Shimadzu UV/vis1601 Spectrophotometer, Japan). The amount of dye adsorption at equilibrium $q_e$ (mg/g) was calculated from the

following equation:

$$q_e = \frac{(C_o - C_e)V}{W} \tag{1}$$

where $C_o$ and $C_e$ (mg/L) are the liquid phase concentrations of dye at initial and equilibrium, respectively, $V$ (L) the volume of the solution and $W$ (g) is the mass of adsorbent used.

The procedure of kinetic tests was basically identical to those of equilibrium tests. The aqueous samples were taken to preset time intervals and the concentrations of dye were similarly measured. The amount of adsorption at time $t$, $q_t$ (mg/g), was calculated by

$$q_t = \frac{(C_o - C_t)V}{W} \tag{2}$$

### 2.4. Effect of initial concentration and contact time

0.30 g sample of GP was added to each 100 mL volume of MB solution. The initial concentrations of dye solution tested were 25, 50, 100, 150 and 200 mg/L and the experiments were carried out at 303 K for 210 min.

### 2.5. Effect of temperature

0.30 g sample of GP was added to each 100 mL volume of MB aqueous solution at different initial concentrations. The experiments were carried out at 303, 313 and 323 K for 210 min.

### 2.6. Effect of solution pH

Effect of solution pH was investigated at pH 4, 6, 8, 10 and 12. 0.30 g sample of GP was added to each 100 mL volume of MB aqueous solution having an initial concentration of 100 mg/L for a constant adsorption time of 210 min.

## 3. Results and discussion

### 3.1. Characterization of GP adsorbent

The BET surface area, total pore volume and average pore diameter of the GP were found to be 0.561 m²/g, 1.12 m³/g and 7.96 nm, respectively. The FTIR analysis is shown in Table 2. The spectra display a number of absorption peaks, indicating the complex nature of the material examined (figure not shown). The FTIR analysis indicated broad bands at 3567 cm$^{-1}$, representing bonded —OH groups. The peak around 1635 cm$^{-1}$ correspond to the C=O stretch. The bands observed at about 831 cm$^{-1}$ could be assigned to the aliphatic C—H group. As seen in Table 2, the spectral analysis before and after dye adsorption indicated that —OH groups, C=O stretching, C—O stretching and C—OH stretching groups were especially involved in MB adsorption. Fig. 1 shows the SEM micrograph of GP sample before and after dye adsorption. The surface of dye-loaded adsorbent (Fig. 1(b)) is different from the surface of adsorbent before adsorption (Fig. 1(a)).

## Table 2
The FTIR spectral characteristics of GP before and after adsorption

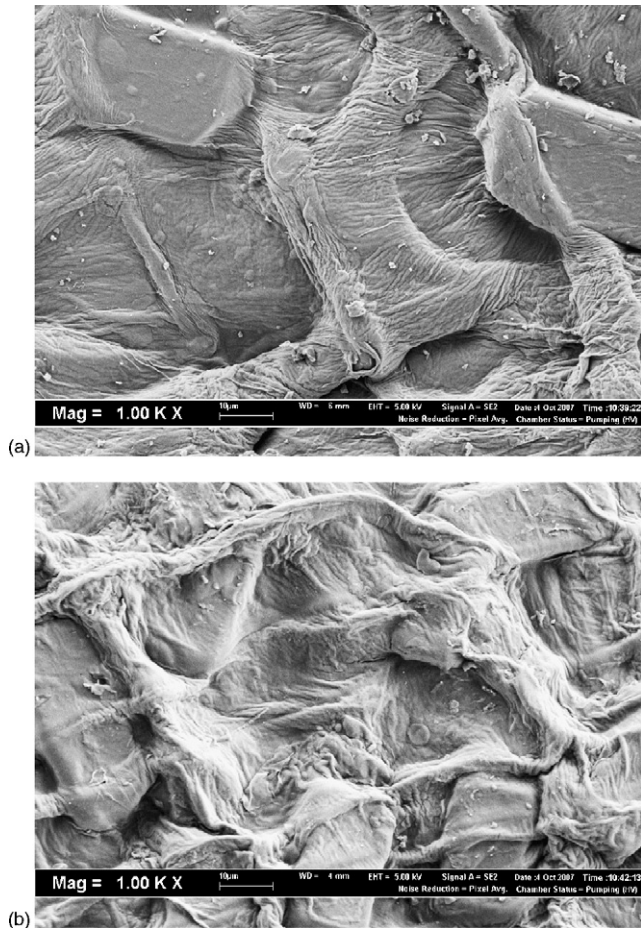| IR peak | Frequency (cm$^{-1}$) | | | Assignment |
|---|---|---|---|---|
| | Before adsorption | After adsorption | Differences | |
| 1 | 3567 | 3546 | −21 | Bonded —OH groups |
| 2 | 1635 | 1631 | −4 | C=O stretching |
| 3 | 1433 | 1440 | +7 | C—O stretching of ether groups |
| 4 | 1069 | 1055 | −14 | —OH stretching vibrations |
| 5 | 831 | 830 | −1 | C—H out-of-plane deformation |

**Fig. 1.** SEM micrograph of the particles of GP (a) before (b) after MB adsorption (magnification: 1000×).

### 3.2. Effects of initial dye concentration and contact time

Fig. 2 shows the adsorption uptake versus the adsorption time at various initial MB concentrations at 303 K. The amount of dye adsorbed (mg/g) increased with increase in time and then reached equilibrium. The amount of dye removed at equilibrium increased from 7.97 to 57.91 mg/g with the increase in dye concentration from 25 to 200 mg/L. It is clear that the removal of dye depends on the concentration of the dye. The initial dye concentration provides the
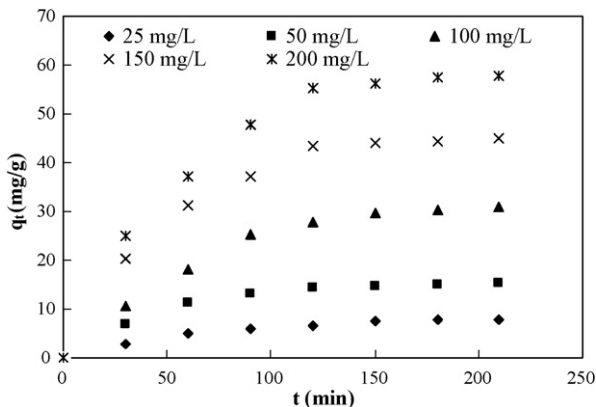


**Fig. 2.** The variation of adsorption capacity with adsorption time at various initial MB concentrations ($T$ = 303 K, $W$ = 0.30 g, $V$ = 100 mL).
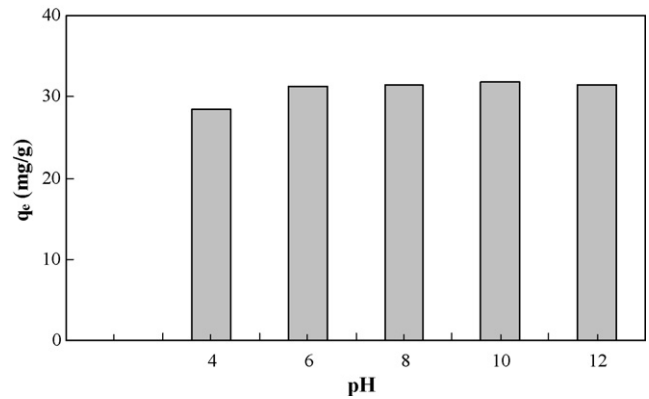


**Fig. 3.** Effect of pH on the adsorption of MB onto GP ($T$ = 303 K, $C_o$ = 100 mg/L, $W$ = 0.30 g, $V$ = 100 mL, contact time = 210 min).

necessary driving force to overcome the resistances to the mass transfer of MB between the aqueous and solid phases [19]. A similar phenomenon was observed for the adsorption of methylene dye onto banana stalk waste [20], pomelo (*C. grandis*) peel [12] and castor seed shell [21].

The adsorption of MB on GP was also studied as a function of contact time in order to find out the equilibrium time for maximum adsorption. The results show that equilibrium time required for the adsorption of MB on GP range from 60 to 90 min for solutions with initial dye concentrations of 25–50 mg/L. However, more than 130 min for MB solutions within initial dye concentrations of 100–200 mg/L. The samples were left for 210 min to ensure equilibrium. An equilibrium adsorption time of 135 min was reported for the adsorption of methylene blue onto wheat shells [22] and 150 min for the adsorption of methylene blue on fallen phoenix tree's leaves [23].

### 3.3. Effect of solution pH on dye adsorption

The pH of dye solution plays an important role in the whole adsorption process, particularly on adsorption capacity [2]. The effect of pH on the adsorption of MB at equilibrium ($q_e$) by GP is shown in Fig. 3. The $q_e$ was found to increase with increasing pH. Lower adsorption at acid pH was probably due to the presence of excess of $H^+$ ions competing with the dye cations for adsorption sites. At higher pH values (6–12) the dye adsorption was almost constant. The surface of GP may contain a large number of active sites, and the solute (dye) uptake can be related to the active sites and also to the chemistry of the solute in the solution. At higher pH, the surface of GP particles may become negatively charged, which enhances the positively charged MB cations through electrostatic forces of attraction [2]. Similar trend was observed for adsorption of methylene blue onto *Posidonia oceanica* (L.) fibres [24], yellow passion fruit peel [25] and methyl violet onto sunflower seed hull [26].

### 3.4. Effect of temperature on dye adsorption

The effect of temperature on the adsorption rate of MB on GP was investigated at 303, 313, and 323 K. Increasing the temperature is known to increase the rate of diffusion of the adsorbate molecules across the external boundary layer and in the internal pores of the adsorbent particle, owing to the decrease in the viscosity of the solution. In addition, changing temperature will change the equilibrium capacity of the adsorbent for a particular adsorbate [11]. The adsorption capacity increased from 82.64 to 142.86 mg/g when temperature of the solution was increased from 303 to 323 K, indi-

**Table 3**
Isotherm parameters for removal of MB by GP different temperatures

| Isotherms | Parameters | Temperatures (K) | | |
|---|---|---|---|---|
| | | 303 | 313 | 323 |
| Langmuir | $Q_o$ (mg/g) | 82.64 | 123.45 | 142.86 |
| | $b$ (L/mg) | 0.085 | 0.044 | 0.05 |
| | $R^2$ | 0.98 | 0.93 | 0.97 |
| Freundlich | $K_F$ (mg/g(L/mg)$^{1/n}$) | 7.88 | 6.297 | 6.79 |
| | $n$ | 1.57 | 1.326 | 1.24 |
| | $R^2$ | 0.99 | 0.99 | 0.99 |
| Temkin | $K_t$ | 11.95 | 10.37 | 4.95 |
| | $B$ | 15.88 | 18.71 | 20.66 |
| | $R^2$ | 0.96 | 0.93 | 0.96 |

cating the process to be endothermic (Table 3). This may be a result of increase in the mobility of the dye with increasing temperature. An increasing number of molecules may also acquire sufficient energy to undergo an interaction with active sites at the surface. Furthermore, increasing temperature may produce a swelling effect within the internal structure of the GP enabling large dye to penetrate further [27].

### 3.5. Adsorption equilibrium

The adsorption isotherm indicates how the adsorption molecules distribute between the liquid phase and the solid phase when the adsorption process reaches an equilibrium state. The analysis of the isotherm data by fitting them to different isotherm models is an important step to find the suitable model that can be used for design purpose [28]. The isotherm data were fitted to the Langmuir, Freundlich and Temkin isotherms.

The Langmuir isotherm [29] is represented by the following linear equation:

$$\frac{C_e}{q_e} = \frac{1}{Q_o b} + \left(\frac{1}{Q_o}\right) C_e \tag{3}$$

where $C_e$ (mg/L) is the equilibrium concentration, $q_e$ (mg/g) the amount of adsorbate adsorbed per unit mass of adsorbate, and $Q_o$ and $b$ are the Langmuir constants related to adsorption capacity and rate of adsorption, respectively. When $C_e/q_e$ was plotted against $C_e$, straight line with slope $1/Q_o$ was obtained (Fig. 4), indicating that the adsorption of MB on GP follows the Langmuir isotherm. The Langmuir constants $b$ and $Q_o$ were calculated from this isotherm and their values are listed in Table 3.

The essential characteristics of Langmuir isotherm can be expressed by a dimensionless constant called equilibrium param-
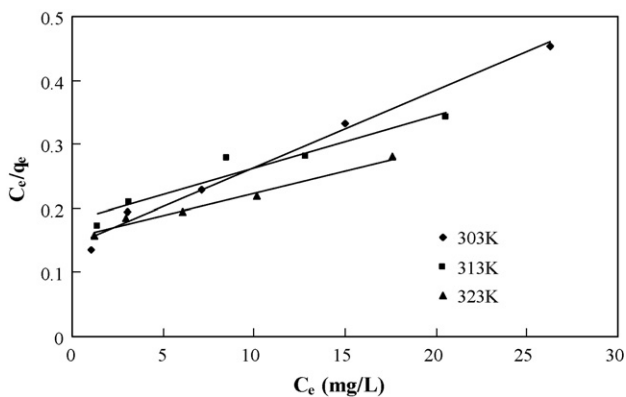


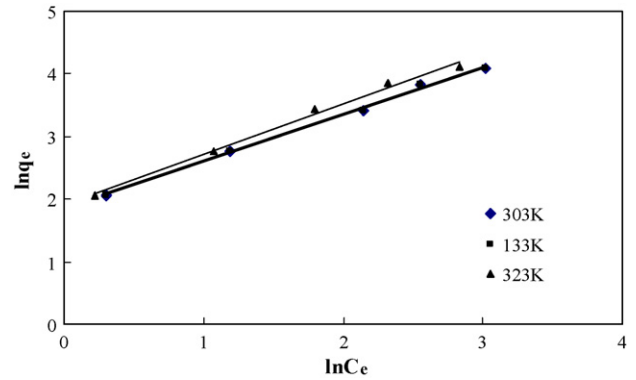**Fig. 4.** Langmuir isotherms for MB dye adsorption onto GP at different temperatures.



**Fig. 5.** Freundlich isotherms for MB dye adsorption onto GP at different temperatures.

eter $R_L$, defined by [30]

$$R_L = \frac{1}{1 + bC_o} \tag{4}$$

where $b$ is the Langmuir constant and $C_o$ (mg/L) is the highest dye concentration. The value of $R_L$ indicates the type of the isotherm to be either unfavorable ($R_L > 1$), linear ($R_L = 1$), favorable ($0 < R_L < 1$) or irreversible ($R_L = 0$). Values of $R_L$ were found to be 0.05, 0.102 and 0.09 at 303, 313 and 323 K, respectively and confirmed that the GP is favorable for adsorption of MB dye under conditions studied.

The linear form of the Freundlich equation [31] is

$$\ln q_e = \ln K_F + \frac{1}{n} \ln C_e \tag{5}$$

where $q_e$ is the amount adsorbed at equilibrium (mg/g) and $C_e$ is the equilibrium concentration of the MB. $K_F$ and $n$ are Freundlich constants, $n$ giving an indication of how favorable the adsorption process and $K_F$ (mg/g(L/mg)$^{1/n}$) is the adsorption capacity of the adsorbent. The slope $1/n$ ranging between 0 and 1 is a measure of adsorption intensity or surface heterogeneity, becoming more heterogeneous as its value gets closer to 0 [32]. The plot of $\ln q_e$ versus $\ln C_e$ (Fig. 5) gives straight lines with slope $1/n$. Fig. 5 shows that the adsorption of MB also follows the Freundlich isotherm. Accordingly, Freundlich constants ($K_F$ and $n$) were calculated and listed in Table 3.

Temkin isotherm [33] is represented by the following equation:

$$q_e = \frac{RT}{b} \ln(K_t C_e) \tag{6}$$

Eq. (6) can be expressed in its linear form as

$$q_e = B \ln K_t + B \ln C_e \tag{7}$$

where

$$B = \frac{RT}{b} \tag{8}$$

The adsorption data were analyzed according to Eq. (7). A plot of $q_e$ versus $\ln C_e$ (Fig. 6) enables the determination of the isotherm constants $K_t$ and $B$. $K_t$ is the equilibrium binding constant (L/mg) corresponding to the maximum binding energy and constant $B$ is related to the heat of adsorption. The values of the parameters are given in Table 3.

From Table 3, the Freundlich isotherm model yielded the best fit with the highest $R^2$ value (0.99) at all temperatures compared to the other two models. Table 4 lists the comparison of maximum monolayer adsorption capacity of MB onto various adsorbents. It is clear that GP used in this work had a relatively suitable adsorption capacity of 82.64 mg/g if compared to other adsorbents found in the literature.
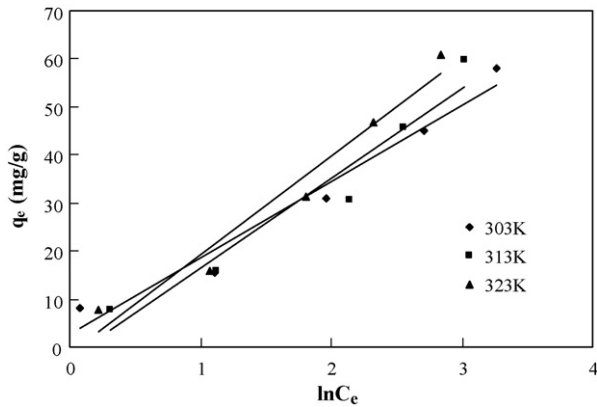
**Fig. 6.** Temkin adsorption isotherm of MB onto GP at different temperatures.

**Table 4**
Comparison of the maximum monolayer adsorption of MB onto various adsorbents

| Adsorbents | Maximum monolayer adsorption capacity (mg/g) | References |
|---|---|---|
| Garlic peel | 82.64 | This work |
| Rice husk | 40.50 | [34] |
| Raw beech sawdust | 9.78 | [35] |
| Oil palm trunk fibre | 149.35 | [36] |
| Broad bean peels | 192.72 | [37] |
| Activated rice husks | 0.21 | [38] |
| Date pits | 80.31 | [39] |
| Jute processing waste | 22.47 | [40] |

## 3.6. Adsorption kinetics

The rate constant of adsorption is determined from the pseudo-first-order rate expression given by Lagergren [41]:

$$\log(q_e - q_t) = \log\ q_e - \left(\frac{k_1}{2.303}\right) t \tag{9}$$

where $q_e$ and $q_t$ (mg/g) are the amounts of dye adsorbed at equilibrium and at time $t$ (min), respectively, and $k_1$ (min$^{-1}$) is the rate constant of adsorption. Values of $k_1$ and $q_e$ were calculated from the plots of $\log(q_e - q_t)$ versus $t$ (Fig. 7) for different initial concentrations of MB are presented in Table 5. It can be seen from Table 5 that the adsorption data were well represented by Lagergren's model with $R^2 \geq 0.92$ for all initial MB concentrations studied.
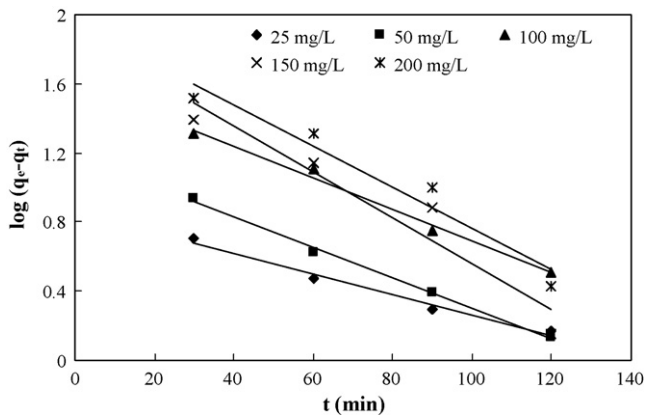
**Table 5**
Kinetic parameters for the removal of MB by GP at 303 K

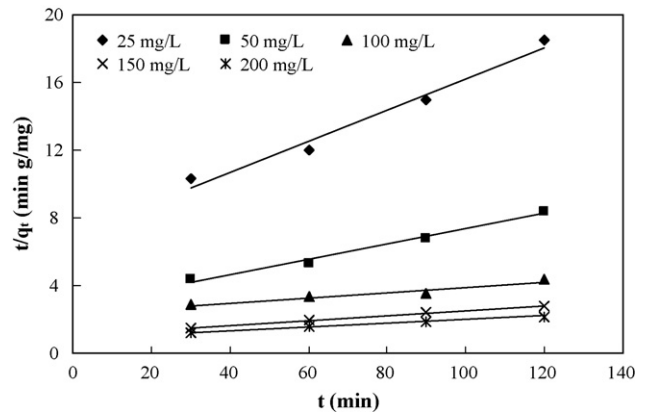| $C_o$ (mg/L) | Pseudo-first-order kinetic | | | Pseudo-second-order kinetic | | |
|---|---|---|---|---|---|---|
| | $q_e$ (mg/g) | $k_1$ (min$^{-1}$) | $R^2$ | $q_e$ (mg/g) | $k_2$ ($\times 10^3$ g/(mg min)) | $R^2$ |
| 25 | 7.18 | 0.014 | 0.98 | 10.89 | 8.42 | 0.98 |
| 50 | 15.51 | 0.021 | 0.99 | 21.88 | 2.13 | 0.99 |
| 100 | 40.45 | 0.021 | 0.98 | 63.69 | 0.24 | 0.95 |
| 150 | 77.19 | 0.031 | 0.92 | 69.93 | 0.21 | 0.99 |
| 200 | 90.65 | 0.027 | 0.94 | 93.45 | 0.11 | 0.99 |



**Fig. 8.** Pseudo-second-order kinetics for adsorption of MB adsorption onto GP at 303 K.

The kinetic data were further analyzed using the pseudo-second-order model [42] expressed as

$$\frac{t}{q_t} = \frac{1}{k_2 q_e^2} + \left(\frac{1}{q_e}\right) t \tag{10}$$

where the equilibrium adsorption capacity ($q_e$), and the pseudo-second-order constants $k_2$ (g/(mg min)) can be determined experimentally from the slope and intercept of plot $t/q_t$ versus $t$ (Fig. 8). The model fits the kinetic date very well with $R^2 \geq 0.95$, which is better than pseudo-first order kinetic (Table 5). These results suggest that the adsorption of MB on GP may be best described by the pseudo-second-order kinetic model with high correlation coefficients.
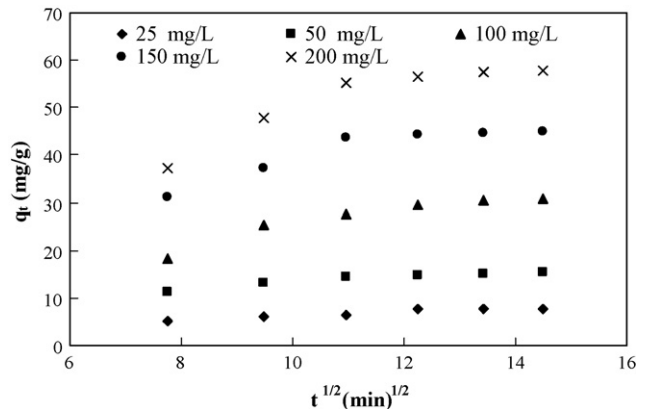


**Fig. 7.** Pseudo-first-order kinetics for adsorption of MB dye onto GP at 303 K.



**Fig. 9.** Weber and Morris intraparticle diffusion plots for removal of MB at different initial dye concentrations.

## 3.7. Intraparticle diffusion

Weber and Moris plot [43] was used to investigate intraparticle diffusion mechanism. The model is

$$q_t = k_i t^{1/2} + C \tag{11}$$

where $k_i$ (mg/g min$^{1/2}$) is intraparticle diffusion rate constant. If intraparticle diffusion is rate-limited then plots of adsorbate uptake $q_t$ versus the square root of time ($t^{1/2}$) would result in a linear relationship and $k_i$ values can be obtained from these plots (Fig. 9). If the regression of $q_t$ versus $t^{1/2}$ is linear and passes through the origin, then intraparticle diffusion is the sole rate-limiting step. However, the linear plots (Fig. 9) at each concentration did not pass through the origin. This indicates that the intraparticle diffusion was not only rate controlling step.

## 4. Conclusions

Garlic peel, an inexpensive and easily available material, was found to very effective to remove MB from aqueous solutions. The equilibrium data were analyzed using the Langmuir, Freundlich, and Temkin isotherm models. The maximum monolayer adsorption capacities were found to be 82.64, 123.45 and 142.86 mg/g at 303, 313 and 323 K, respectively. Equilibrium data fitted very well with Freundlich isotherm equation. The kinetics of the adsorption process was found to follow the pseudo-second-order kinetic model.

## Acknowledgment

## References

[1] G. Renmin, L. Mei, Y. Chao, S. Yingzhi, C. Jian, Removal of cationic dyes from aqueous solution by adsorption on peanut hull, J. Hazard. Mater. B121 (2005) 247–250.
[2] B. Yasemin, A. Haluk, A kinetics and thermodynamics study of methylene blue adsorption on wheat shells, Desalination 194 (2006) 259–267.
[3] J. Panswed, S. Wongchaisuwan, Mechanism of dye wastewater color removal by magnesium carbonate-hydrated basic, Water Sci. Technol. 18 (1986) 139–144.
[4] P.K. Malik, S.K. Saha, Oxidation of direct dyes with hydrogen peroxide using ferrous ion as catalyst, Sep. Purif. Technol. 31 (2003) 241–250.
[5] M. Koch, A. Yediler, D. Lienert, G. Insel, A. Kettrup, Ozonation of hydrolyzed azo dye reactive yellow 84 (CI), Chemosphere 46 (2002) 109–113.
[6] G. Ciardelli, L. Corsi, M. Marucci, Membrane separation for wastewater reuse in the textile industry, Resour. Conserv. Recycl. 31 (2000) 189–197.
[7] F.C. Wu, R.L. Tseng, High adsorption capacity NaOH-activated carbon for dye removal from aqueous solution, J. Hazard. Mater. 152 (2008) 1256–1267.
[8] N. Thinakaran, P. Baskaralingam, M. Pulikesi, P. Panneerselvam, S. Sivanesan, Removal of Acid Violet 17 from aqueous solutions by adsorption onto activated carbon prepared from sunflower seed hull, J. Hazard. Mater. 151 (2008) 316–322.
[9] A.A. Ahmad, B.H. Hameed, N. Aziz, Adsorption of direct dye on palm ash: kinetic and equilibrium modeling, J. Hazard. Mater. 141 (2007) 70–76.
[10] M. Hasan, A.L. Ahmad, B.H. Hameed, Adsorption of reactive dye onto cross-linked chitosan/oil palm ash composite beads, Chem. Eng. J. 136 (2008) 164–172.
[11] Z. Al-Qodah, Adsorption of dyes using shale oil ash, Water Res. 34 (2000) 4295–4303.
[12] B.H. Hameed, D.K. Mahmoud, A.L. Ahmad, Sorption of basic dye from aqueous solution by pomelo (Citrus grandis) peel in a batch system, Colloids Surf. A: Physicochem. Eng. Aspects 316 (2008) 78–84.
[13] A. Mittal, A. Malviya, D. Kaur, J. Mittal, L. Kurup, Studies on the adsorption kinetics and isotherms for the removal and recovery of methyl orange from wastewaters using waste materials, J. Hazard. Mater. 148 (2007) 229–240.
[14] J.F. Osma, V. Saravia, J.L. Toca-Herrera, S.R. Couto, Sunflower seed shells: a novel and effective low-cost adsorbent for the removal of the diazo dye reactive black 5 from aqueous solutions, J. Hazard. Mater. 147 (2007) 900–905.
[15] V.K. Gupta, R. Jain, S. Varshney, V.K. Saini, Removal of Reactofix Navy Blue 2 GFN from aqueous solutions using adsorption techniques, J. Colloid Interf. Sci. 307 (2007) 326–332.
[16] V.K. Gupta, R. Jain, S. Varshney, Removal of Reactofix Golden Yellow 3 RFN from aqueous solution using wheat husk—an agricultural waste, J. Hazard. Mater. 142 (2007) 443–448.
[17] V. Ponnusami, S. Vikram, S.N. Srivastava, Guava (Psidium guajava) leaf powder: novel adsorbent for removal of methylene blue from aqueous solutions, J. Hazard. Mater. 152 (2008) 276–286.
[18] A.K. Jain, V.K. Gupta, A. Bhatnagar, Suhas, Utilization of industrial waste products as adsorbents for the removal of dyes, J. Hazard. Mater. B101 (2003) 31–42.
[19] V.C. Srivastava, M.M. Swamy, I.D. Mall, B. Prasad, I.M. Mishra, Adsorptive removal of phenol by bagasse fly ash and activated carbon: equilibrium, kinetics and thermodynamics, Colloids Surf. A: Physicochem. Eng. Aspect 272 (2006) 89–104.
[20] B.H. Hameed, D.K. Mahmoud, A.L. Ahmad, Sorption equilibrium and kinetics of basic dye from aqueous solution using banana stalk waste, J. Hazard. Mater. 158 (2008) 499–506.
[21] N.A. Oladoja, C.O. Aboluwoye, Y.B. Oladimeji, A.O. Ashogbon, I.O. Otemuyiwa, Studies on castor seed shell as a sorbent in basic dye contaminated wastewater remediation, Desalination 227 (2008) 190–203.
[22] Y. Bulut, H. Aydın, A kinetics and thermodynamics study of methylene blue adsorption on wheat shells, Desalination 194 (2006) 259–267.
[23] R. Han, W. Zou, W. Yu, S. Cheng, Y. Wang, J. Shi, Biosorption of methylene blue from aqueous solution by fallen phoenix trees leaves, J. Hazard. Mater. 141 (2007) 156–162.
[24] M.C. Ncibi, B. Mahjoub, M. Seffen, Kinetic and equilibrium studies of methylene blue biosorption by Posidonia oceanica (L.) fibres, J. Hazard. Mater. B139 (2007) 280–285.
[25] F.A. Pavan, A.C. Mazzocato, Y. Gushikem, Removal of methylene blue dye from aqueous solutions by adsorption using yellow passion fruit peel as adsorbent, Bioresour. Technol. 99 (2008) 3162–3165.
[26] B.H. Hameed, Equilibrium and kinetic studies of methyl violet sorption by agricultural waste, J. Hazard. Mater. 154 (2008) 204–212.
[27] M. Alkan, M. Dogan, Adsorption kinetics of Victoria blue onto perlite, Fresen. Environ. Bull. 12 (2003) 418–425.
[28] M. El-Guendi, Homogeneous surface diffusion model of basic dyestuffs onto natural clay in batch adsorbers, Adsorpt. Sci. Technol. 8 (2) (1991) 217–225.
[29] I. Langmuir, Adsorption of gases on plain surfaces of glass mica platinum, J. Am. Chem. Soc. 40 (1918) 136–403.
[30] T.W. Weber, P. Chakkravorti, Pore and solid diffusion models for fixed-bed adsorbers, AIChE J. (1974) 220–228.
[31] H.M.F. Freundlich, Over the adsorption in solution, J. Phys. Chem. 57 (1906) 385–470.
[32] F. Haghseresht, G. Lu, Adsorption characteristics of phenolic compounds onto coal-reject-derived adsorbents, Energy Fuels 12 (1998) 1100–1107.
[33] M.J. Tempkin, V. Pyzhev, Acta Physiochim. USSR 12 (1940) 217–222.
[34] V. Vadivelan, K. Kumar, Equilibrium, kinetics, mechanism, and process design for the sorption of methylene blue onto rice husk, J. Colloid Interf. Sci. 286 (2005) 90–100.
[35] F.A. Batzias, D.K. Sidiras, Dye adsorption by calcium chloride treated beech sawdust in batch and fixed-bed systems, J. Hazard. Mater. B114 (2004) 167–174.
[36] B.H. Hameed, M.I. El-Khaiary, Batch removal of malachite green from aqueous solutions by adsorption on oil palm trunk fibre: equilibrium isotherms and kinetic studies, J. Hazard. Mater. 154 (2008) 237–244.
[37] B.H. Hameed, M.I. El-Khaiary, Sorption kinetics and isotherm studies of a cationic dye using agricultural waste: broad bean peels, J. Hazard. Mater. 154 (2008) 639–648.
[38] V.K. Gupta, A. Mittal, R. Jain, M. Mathur, S. Sikarwar, Adsorption of Safranin-T from wastewater using waste materials—activated carbon and activated rice husks, J. Colloid Interf. Sci. 303 (2006) 80–86.
[39] F. Banat, S. Al-Asheh, L. Al-Makhadmeh, Evaluation of the use of raw and activated date pits as potential adsorbents for dye containing waters, Proc. Biochem. 39 (2003) 193–202.
[40] S. Banerjee, M.G. Dastidar, Use of jute processing wastes for treatment of wastewater contaminated with dye and other organics, Bioresour. Technol. 96 (2005) 1919–1928.
[41] S. Lagergren, Zur theorie der sogenannten adsorption geloester stoffe, Kungliga Svenska Vetenskapsakad, Handl. 24 (1898) 1–39.
[42] G. McKay, Y.S. Ho, Pseudo-second order model for sorption processes, Process Biochem. 34 (1999) 451–465.
[43] W.J. Weber, J.C. Morris, Kinetics of adsorption on carbon from solution, J. Sanitary Eng. Div. Proc. Am. Soc. Civil Eng. 89 (1963) 31–59.